Supporting Information

Room-temperature conversion of $Cu_{2-x}Se$ to CuAgSe nanoparticles to enhance the photocatalytic performance of their composites with TiO_2

Sweta Gahlot,[1] Frederic Dappozze,[1] Deobrat Singh,[2] Rajeev Ahuja,[2] Luis Cardenas,[1] Laurence Burel,[1] David Amans,[3] Chantal Guillard,[1] Shashank Mishra*[1]

[1]Université Claude Bernard Lyon 1, CNRS, UMR 5256, Institut de Recherches sur la Catalyse et l'Environnement de Lyon (IRCELYON), 2 avenue Albert Einstein, 69626 Villeurbanne, France.

[2] Condensed Matter Theory Group, Department of Physics and Astronomy, Uppsala University, Box 516, 75120 Uppsala, Sweden.

[3] Université Claude Bernard Lyon 1, CNRS, Institut Lumière Matière (ILM), 69626 Villeurbanne, France.

E-mail : shashank.mishra@ircelyon.univ-lyon1.fr (SM)

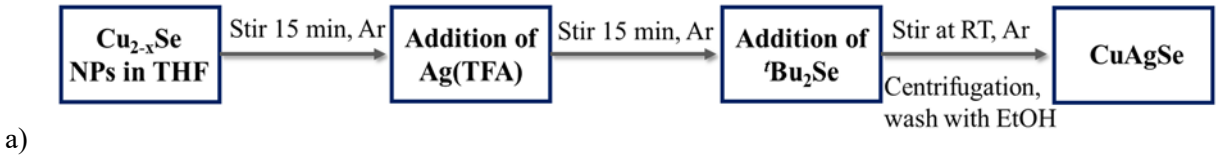

a)

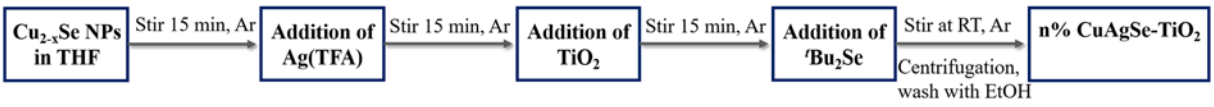

b)

Figure S1. Schematic representation of the synthesis of the a) CuAgSe NPs and b) *n*% CuAgSe-TiO_2 nanocomposites.

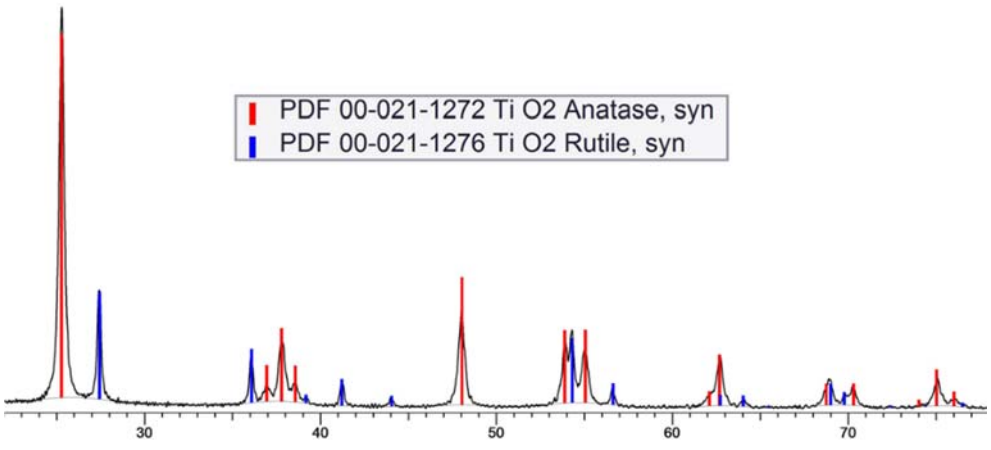

a)

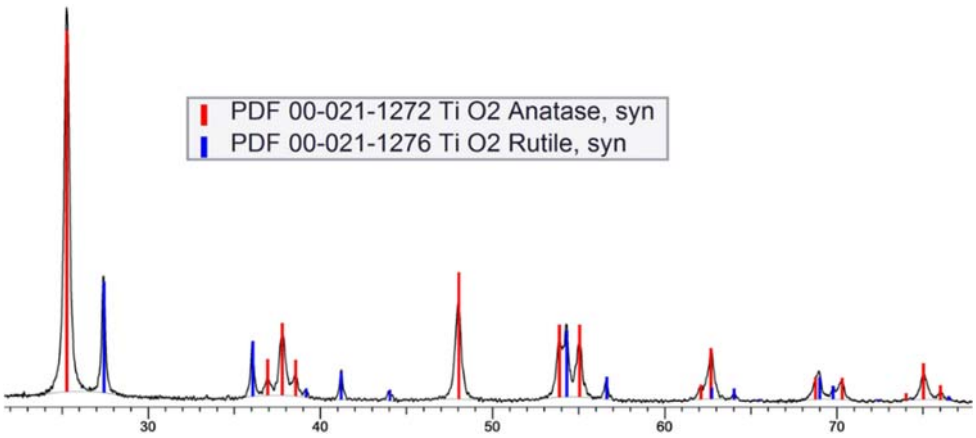

b)

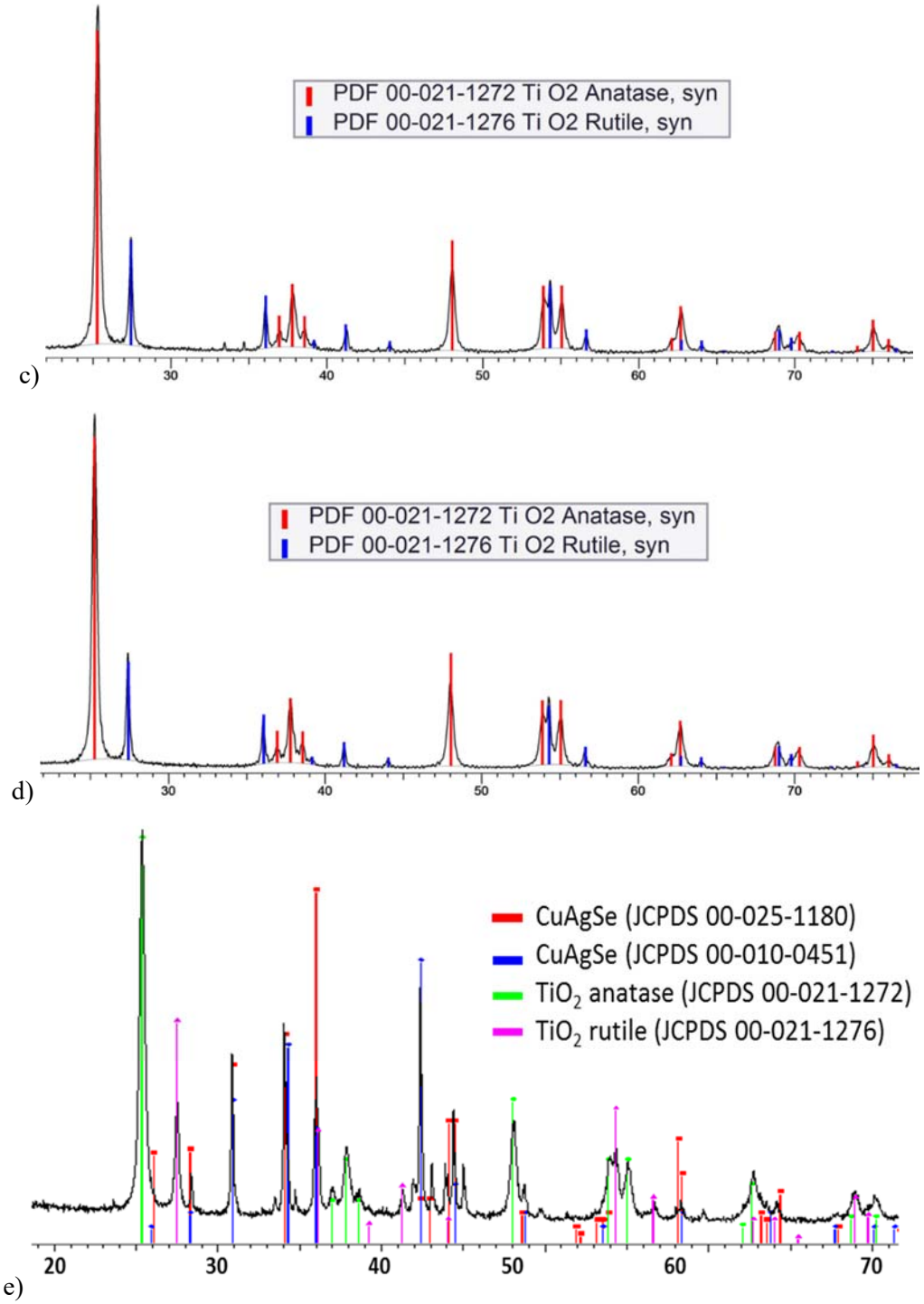

Figure S2. XRD patterns of n mol% CuAgSe-TiO_2 nanocomposites obtained from $Cu_{2-x}Se$, Ag(TFA), $^tBu_2Se$ and TiO_2 when stirred at room temperature for 6h. (a) 0.01% CuAgSe-TiO_2, (b) 0.1% CuAgSe-TiO_2, (c) 0.3% CuAgSe-TiO_2, (d) 1% CuAgSe-TiO_2, and (e) 10% CuAgSe-TiO_2.

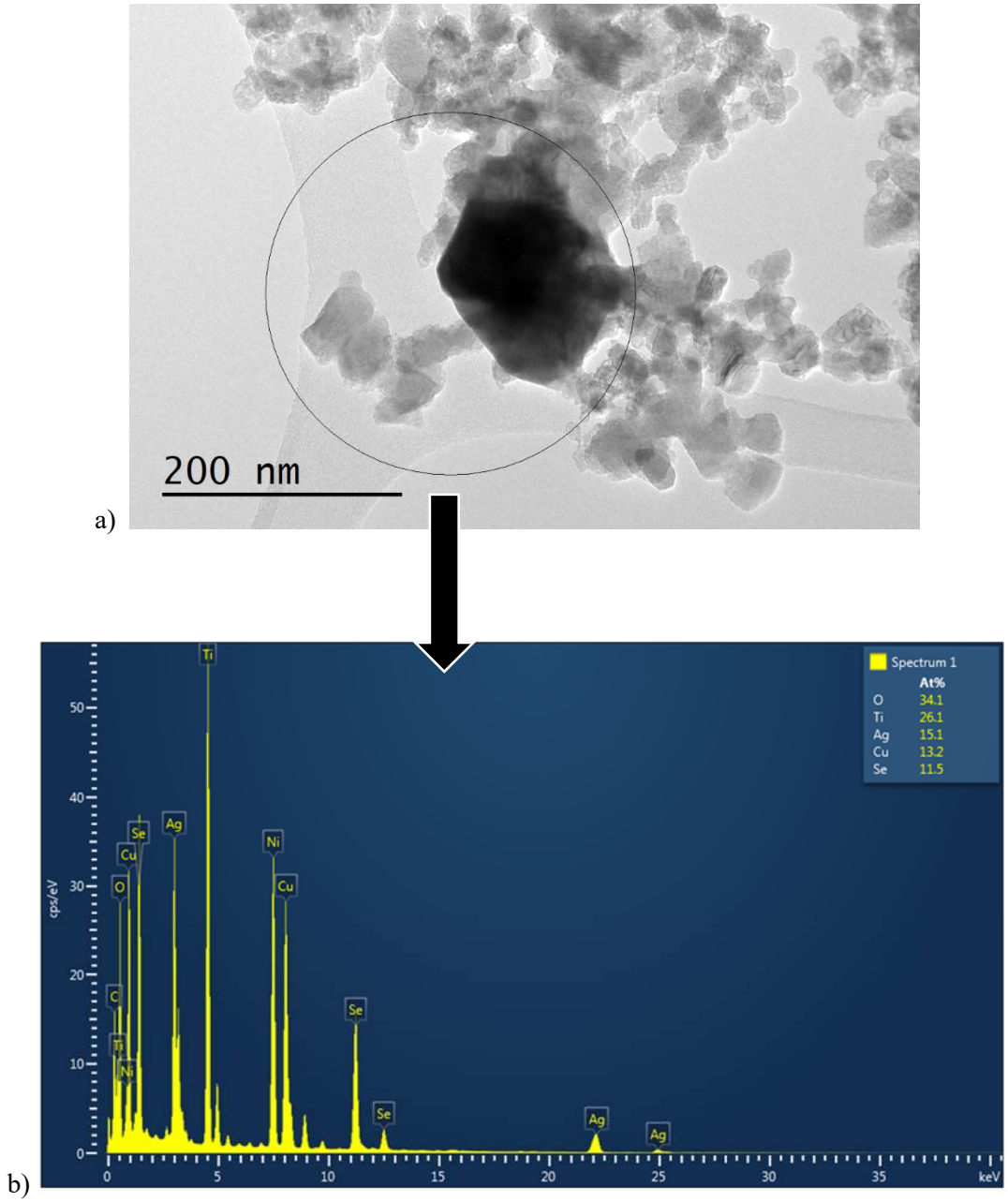

Figure S3. TEM image (a) and associated EDX analysis (b) of 10% CuAgSe-TiO_2 nanocomposites.

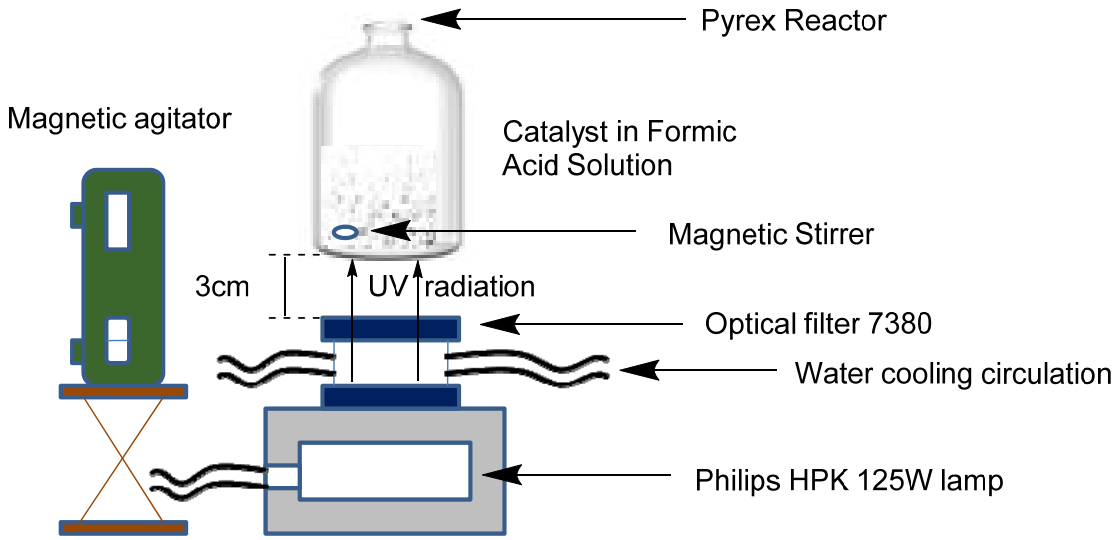

Figure S4. The experimental setup for FA photodegradation under UV light.

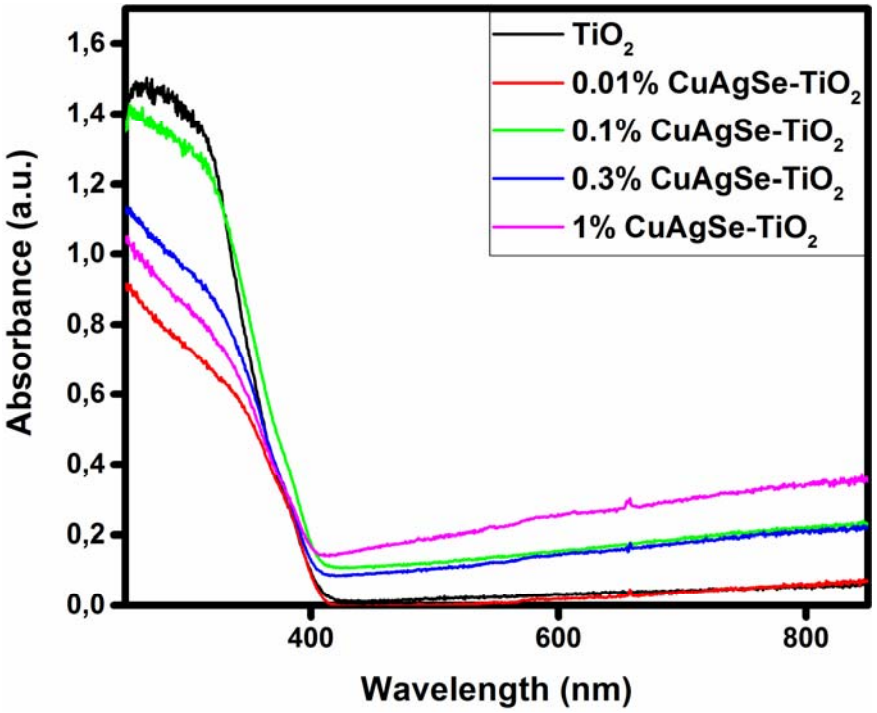

Figure S5. Absorbance spectra for n% CuAgSe-TiO_2 nanocomposites.

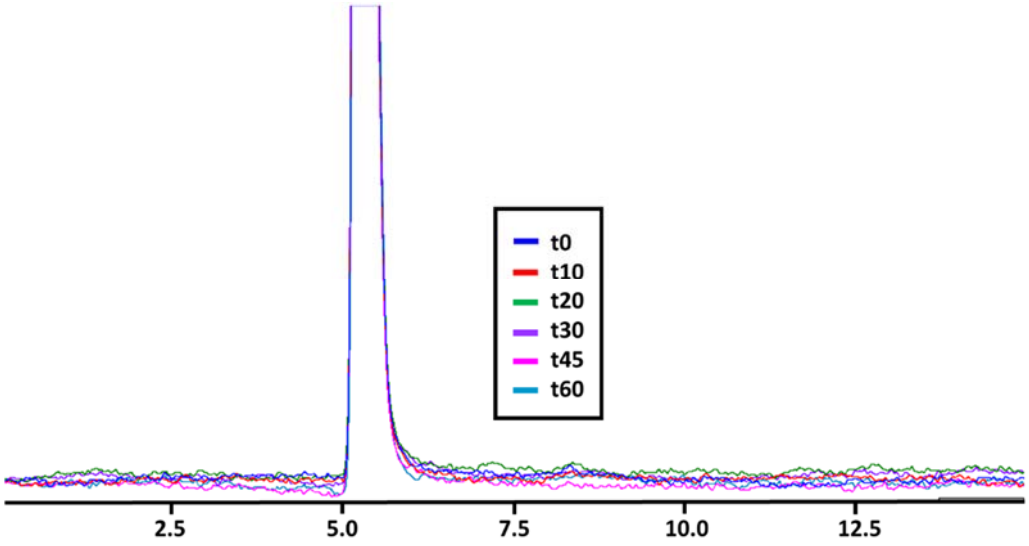

Figure S6. HPLC result after stability test using 0.3% CuAgSe-TiO_2 under acidic conditions (HNO_3).

Table S1. N_2 adsorption and desorption isotherm and related data of TiO_2 and CuAgSe-TiO_2 nanocomposites.

Sample Name	Surface area (m^2/g)	Total pore volume (cm^3/g)	Av. Pore diameter (nm)
TiO_2	58.9	0.23	15.6
0.01% CuAgSe-TiO_2	53.7	0.52	38.9
0.1% CuAgSe-TiO_2	52.4	0.49	37.5
0.3% CuAgSe-TiO_2	51.2	0.41	32
1% CuAgSe-TiO_2	54.9	0.24	17.6